

# Reading, Not Thinking: Understanding and Bridging the Modality Gap When Text Becomes Pixels in Multimodal LLMs

Kaiser Sun<sup>1\*</sup>, Xiaochuang Yuan<sup>2\*</sup>, Hongjun Liu<sup>3\*</sup>,  
Chen Zhao<sup>3</sup>, Cheng Zhang<sup>4</sup>, Mark Dredze<sup>1</sup>, and Fan Bai<sup>1</sup>

<sup>1</sup> Johns Hopkins University

<sup>2</sup> Amazon

<sup>3</sup> New York University

<sup>4</sup> Texas A&M University

**Abstract.** Multimodal large language models (MLLMs) can process text presented as images, yet they often perform worse than when the same content is provided as textual tokens. We systematically diagnose this “modality gap” by evaluating seven MLLMs across seven benchmarks in five input modes, spanning both synthetically rendered text and realistic document images from arXiv PDFs to Wikipedia pages. We find that the modality gap is task- and data-dependent. For example, math tasks degrade by over 60 points on synthetic renderings, while natural document images often match or exceed text-mode performance. Rendering choices such as font and resolution are strong confounds, with font alone swinging accuracy by up to 47 percentage points. To understand this, we conduct a grounded-theory error analysis of over 4,000 examples, revealing that image mode selectively amplifies reading errors (calculation and formatting failures) while leaving knowledge and reasoning errors largely unchanged, and that some models exhibit a chain-of-thought reasoning collapse under visual input. Motivated by these findings, we propose a self-distillation method that trains the model on its own pure text reasoning traces paired with image inputs, raising image-mode accuracy on GSM8K from 30.71% to 92.72% and transferring to unseen benchmarks without catastrophic forgetting. Overall, our study provides a systematic understanding of the modality gap and suggests a practical path toward improving visual text understanding in multimodal language models.

## 1 Introduction

Humans read text through vision: we perceive words as visual patterns on pages, screens, and signs, not as sequences of abstract symbols [16, 17]. Modern multimodal large language models (MLLMs), however, process text and images through separate pathways, compressing visual input into tokens before fusing it with textual representations [1, 3, 9, 25, 36]. When the same textual content is presented as an image rather than as text tokens, these models often produce different, and frequently worse, predictions (Figure 1). This “modality

---

\* Equal contribution

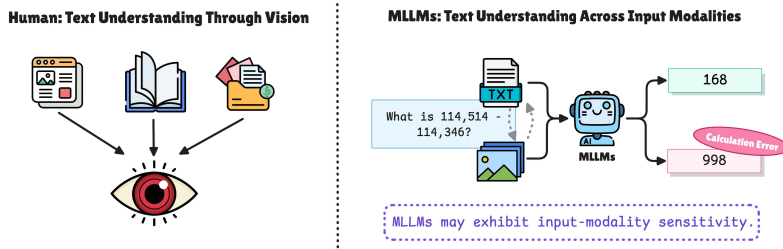


**Fig. 1:** Humans read text through vision from diverse sources such as books, webpages, and documents, whereas MLLMs may yield different predictions when the same textual content is presented in different input forms.

gap” has been documented across math, coding, and knowledge tasks [27, 35], and motivates a growing line of work on visual text processing, including screenshot language models [18, 32], vision-centric tokenization [10, 43], and unified multimodal architectures [40].

Yet existing work predominantly focuses on either *documenting* the gap or *building new systems* to circumvent it, without systematically explaining *why* the gap arises in current MLLMs, characterizing *when* visual input helps versus hinders, or showing *how* the gap can be closed with minimal intervention. A further limitation is that existing evaluations rely almost exclusively on *synthetically rendered* text images, potentially confounding rendering artifacts with genuine perceptual deficits.

In this work, we diagnose the modality gap and show it can be substantially narrowed. We evaluate seven MLLMs across seven benchmarks in five input modes (Figure 2), spanning synthetically rendered text and realistic document images from arXiv PDFs and Wikipedia pages. Two OCR-based modes decompose the visual pipeline into reading and reasoning stages, isolating their respective contributions to the gap.

We find that the gap is task- and data-dependent, not universal. On synthetic benchmarks, math tasks show gaps exceeding 60 points while knowledge-intensive tasks show modest drops. On natural document images, MLLMs often *match or exceed* their text-mode performance, suggesting the gap partly reflects distributional mismatch between synthetic renderings and pretraining data. Consistent with this, rendering choices turn out to be a critical confound: font choice alone swings accuracy by up to 47%, and resolution sensitivity varies dramatically across architectures.

To understand *why* image mode degrades performance, we conduct a grounded-theory error analysis of over 4,000 errors. The taxonomy reveals that image mode selectively amplifies perceptual errors (calculation and format errors increase by  $1.5\times$ ) while leaving conceptual and reasoning errors largely unchanged. We also identify a chain-of-thought reasoning collapse, where models produce dramatically shorter outputs in image mode, bypassing step-by-step reasoning. Together, these findings establish that *image mode impairs reading, not thinking*.

Motivated by this diagnosis, we propose a self-distillation approach: training the model on its own text-mode reasoning traces paired with image inputs. This

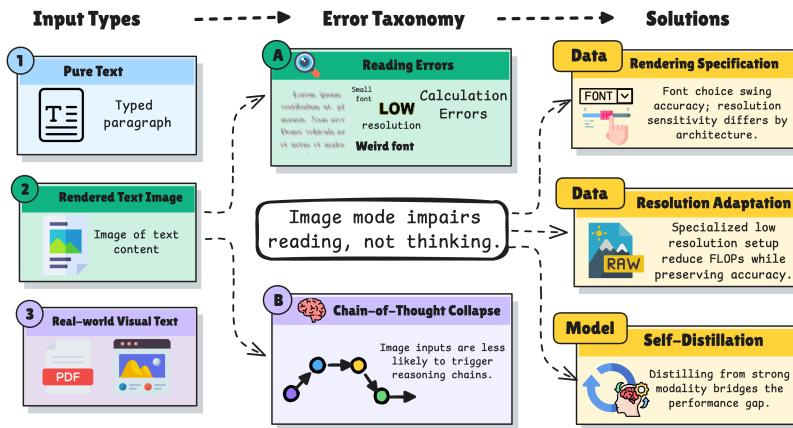


**Fig. 2:** Diagnosing the modality gap in visual text understanding. We evaluate MLLMs across five input modes, including pure text, rendered text images, real-world visual text, and two OCR-based diagnostic settings (OCR-1P and OCR-2P). Our error taxonomy reveals that while image modality amplifies reading and calculation errors, it leaves underlying reasoning capabilities largely intact but also reduces the likelihood of triggering a reasoning chain. We further propose remedies to bridge the performance gap, including rendering specification control, resolution-aware preprocessing, and LM-only self-distillation.

raises image-mode accuracy on GSM8K from 30.71% to 92.72%, nearly matching text-mode performance. Both vision encoder and language model adaptation contribute, with the language model playing a larger role, and the gains transfer to unseen benchmarks without catastrophic forgetting.

## 2 Related Work

*Visual Text Processing.* A growing body of work explores processing language through visual representations rather than discrete tokens. Screenshot language models [18, 32] train vision transformers on rendered text with masked patch prediction, progressively closing the gap with text-only models such as BERT on standard NLU benchmarks. On the efficiency front, vision-centric tokenization methods render text as images to reduce token counts: SeeTok [43] achieves competitive performance with  $4.43\times$  fewer tokens, while Glyph [10] demonstrates  $3\text{--}4\times$  context compression via continual pre-training with rendering search. At the architectural level, Emu3 [40] shows that a single decoder-only transformer performing next-token prediction over a shared discrete space of images, text, and video can match compositional encoder-LLM architectures, establishing unified token prediction as a viable foundation for multimodal learning. These works focus on *building better systems*, including new training objectives, tokenization schemes, and unified architectures. In contrast, our work takes existing MLLMs as given and first diagnoses *why* they fail when reading text as images, then

shows that the gap can be narrowed with minimal, targeted training rather than architectural redesign.

*Evaluating MLLMs on Visual Text.* Unlike scene-text understanding [5, 33, 34], which primarily tests text recognition in natural images, recent work has turned to evaluating whether MLLMs can *reason* over textual content presented visually, documenting a “modality gap” between text and image presentation. PixelWorld [27] reports that the gap is task-dependent: semantic tasks are largely preserved while math and coding degrade. VISTA-Bench [26] evaluates over 20 VLMs across perception, reasoning, and knowledge tasks. Li et al. [24] show that rendering long contexts as images can halve decoder token counts while maintaining accuracy on retrieval and summarization. Most closely related, Sprang et al. [35] introduce the REST benchmarks to measure *cross-modal consistency*, i.e., whether models produce the same answer regardless of input modality, finding at least  $\sim 10\%$  inconsistency across all models and that visual characteristics such as resolution and colour affect consistency. These evaluations predominantly rely on *synthetically rendered* text images, which may confound rendering artifacts with genuine perceptual deficits. Our work complements this literature by including realistic image benchmarks (SQuAD [30] and QASPER [15]) from natural sources (Wikipedia screenshots and arXiv PDF pages), showing that rendering choices such as font can swing accuracy by 47 pp. We further *explain* the gap through an error taxonomy that separates reading failures from knowledge and reasoning failures, showing that image mode selectively amplifies reading errors while leaving reasoning errors invariant.

*Closing the Modality Gap.* While the works above establish that a text-versus-image gap exists, relatively little work addresses *how to close it* in existing MLLMs. Wang et al. [41] demonstrate that embedding text in images produces divergent effects across architectures (Qwen2.5-VL improves while LLaVA collapses), tracing the difference to vision encoder design, but do not propose a general remedy. Hu et al. [23] show that visual priors alone (2D positional embeddings, canvas augmentation) can achieve competitive performance on ARC, suggesting that visual representations carry complementary information to symbolic tokens, but this requires training a model from scratch. Our self-distillation experiments offer a different perspective: by training the model on its own text-mode reasoning traces paired with image inputs, we show that the modality gap can be substantially narrowed, with both vision encoder and language model adaptation contributing. This connects to the broader literature on cross-modal knowledge distillation [19, 37], but differs in that the teacher and student are the *same* model operating in different modalities: the model distills its own text-mode competence into its visual-input pathway.

### 3 Evaluation Setup

#### 3.1 Datasets

As discussed in Section 2, our focus is on *reasoning* over visually presented text rather than scene-text recognition. We include the following datasets:

*Synthetic-image datasets.* Five benchmarks from prior visual text evaluations exhibit clear modality gaps, allowing us to examine their source. **MMLU** [20, 21] contains multiple-choice questions across 57 knowledge domains. **ARC** [11] includes challenging grade-school science questions. **GPQA (Diamond)** [31] is the most stringently filtered GPQA subset, containing 198 graduate-level science questions that experts answer correctly but non-experts often fail. **GSM8K** [13] consists of grade-school math word problems. **HumanEval** [7] evaluates Python code generation from natural-language descriptions. Because these tasks are purely textual, their image counterparts are synthetically rendered.

*Natural-image datasets.* Synthetic renderings may not reflect the visual distribution of real-world text. We therefore include two datasets whose image inputs come from natural sources. **QASPER** [15] is a long-form QA dataset over scientific articles that often requires long context reasoning.<sup>5</sup> We obtain the original PDF files from arXiv and convert relevant pages into PNG images using the *fitz* library.<sup>6</sup> **SQuAD (v2)** [29] is an extractive QA dataset built over Wikipedia. For each example, we capture a screenshot of the corresponding Wikipedia page to create a natural-image version of the context. Additional details on dataset processing and image construction are provided in the appendix.

*Evaluation metrics.* We follow the standard metric for each dataset, using pass@k for HumanEval and accuracy for the rest. For QASPER and SQuAD, zero-shot MLLM inference does not align well with span-based metrics, because MLLMs are not trained to reproduce annotation artifacts such as exact spans. Following recent information-seeking benchmarks [28, 42], we adopt an LLM-as-judge protocol, where we use GPT-5 (*gpt-5-2025-08-07*) to compare the model prediction with the gold answer and report accuracy. Results using span-based F1 are provided in the appendix.

### 3.2 Input Modalities

We compare five input modalities, with examples shown in the appendix. Prior work has examined **Pure Text**, **Pure Image**, and **Instr.+Image** separately; we place them in a unified comparison and additionally introduce two OCR-based settings that help isolate whether the modality gap stems from failures in *reading* text from pixels, failures in *reasoning* over the extracted content, or both.

*Pure Text.* The model receives only the original textual content (e.g., question, answer options, passages, or function signatures), preceded by a task instruction when necessary. This serves as our reference modality. *Pure Image.* The identical textual content from **Pure Text** is rendered into a 1280×720 image (white canvas, black text) following prior work [12, 27]; the model receives only this image. For natural-image datasets, the task instruction is rendered and concatenated at the top of the document image. Section 4 examines how rendering parameters (font, resolution, compression) affect performance.

<sup>5</sup> We remove questions that depend on tables and figures for a fair comparison across modalities. Results on the full test set are in the appendix.

<sup>6</sup> <https://pypi.org/project/fitz/>

*Instr.+Image*. The model receives the example content as an image and the task instruction as text. This setting closely mirrors traditional VQA-style inputs, where language instructions are provided textually while the model must read text embedded in the image.

*OCR-1P (one pass)*. The model receives the same image as in *Instr.+Image*, but the instruction explicitly asks it to first extract all text from the image and then solve the task, all within a single inference pass. This tests whether explicitly prompting for text extraction improves downstream performance while still coupling reading and reasoning.

*OCR-2P (two passes)*. In this two-stage pipeline, the model first receives the image and is prompted *only* to extract the textual content. The extracted text is then fed back into the model as a new **Pure Text** query to solve the task. By fully separating reading from reasoning, this setting isolates whether errors originate from the vision-based text extraction or from downstream task execution.

### 3.3 Models

We evaluate seven MLLMs selected to span different architectures, model scales, and access types. Our selection includes six open-source models: Qwen2.5-VL (7B and 32B) [4], Qwen3-VL-8B [44], InternVL3-8B [8], InternVL3.5-8B [39], and Pixtral-12B [2], as well as the proprietary GPT-5.2 (*gpt-5.2-2025-12-11*). The open-source models share a common architecture in which a ViT-based visual encoder converts input images into visual tokens that are fed into an autoregressive LLM decoder. All models receive identical inputs for each modality, and inference parameters are listed in the appendix.

## 4 Results

### 4.1 Modality Gap on Synthetic and Natural Images

*Performance on synthetic images*. Tab. 1 reports results on five synthetic-image datasets, with cell shading indicating the performance difference relative to **Pure Text** (red = better than text, blue = worse). On MMLU and GPQA, **Pure Text** dominates for nearly every model, while **Pure Image** lags by 1–8 points. On ARC, models still perform better on text, but the gap narrows: Qwen2.5-VL-7B achieves 89.42% under **Pure Image**, and InternVL3.5-8B ties its text baseline. HumanEval exhibits strong model-dependent behavior. GPT-5.2 and InternVL3.5-8B retain near-full performance across modalities, while Qwen2.5-VL-32B shows a surprising inversion: **Pure Text** yields only 31.10 whereas **Pure Image** reaches 85.98, suggesting that this model’s text-mode code generation may be miscalibrated rather than that image input is inherently superior. GSM8K

<sup>7</sup> OCR-2P is omitted for QASPER due to the computational cost of running OCR on extremely long documents. Pixtral-12B is excluded from QASPER due to insufficient context length.

Dataset	Model	Pure Instr.+		Pure Image	OCR-1P	OCR-2P	Dataset	Model	Pure Instr.+		Pure Image	OCR-1P	OCR-2P
		Text	Image						Text	Image			
		(T)	(T+I)	(I)	(T→I)	(I→T)			(T)	(T+I)	(I)	(T→I)	(I→T)
MMLU	GPT-5.2	92.33	91.06	90.93	86.54	86.72	Human Eval	GPT-5.2	100.00	71.34	100.00	98.17	100.00
	InternVL3-8B	59.83	69.09	33.93	0.37	71.86		InternVL3-8B	56.71	71.95	45.12	0.00	0.00
	InternVL3.5-8B	63.97	63.70	62.27	68.99	80.75		InternVL3.5-8B	90.24	90.24	89.02	84.76	86.59
	Pixtral-12B	37.89	41.60	42.76	0.66	44.25		Pixtral-12B	39.02	79.27	47.56	0.00	0.00
	Qwen2.5-7B-VL	67.80	67.97	67.36	34.44	67.08		Qwen2.5-7B-VL	59.15	83.54	65.24	0.00	64.02
	Qwen2.5-32B-VL	78.34	75.47	73.79	76.55	80.38		Qwen2.5-32B-VL	31.10	22.56	85.98	0.00	82.32
Qwen3-8B	78.44	72.29	71.01	34.45	73.61	Qwen3-8B	76.22	82.93	82.93	0.00	0.00		
ARC	GPT-5.2	97.70	92.24	95.48	97.70	97.18	GSM8K	GPT-5.2	95.83	85.14	96.51	77.86	68.16
	InternVL3-8B	92.24	91.30	90.27	0.00	70.73		InternVL3-8B	78.01	49.51	42.53	0.00	87.87
	InternVL3.5-8B	92.66	92.41	92.66	66.04	71.93		InternVL3.5-8B	95.30	95.22	95.30	87.64	94.47
	Pixtral-12B	84.64	71.25	61.77	0.00	38.74		Pixtral-12B	3.79	4.93	8.11	0.00	55.12
	Qwen2.5-7B-VL	87.20	85.92	89.42	34.47	66.55		Qwen2.5-7B-VL	19.48	20.24	24.79	18.50	20.17
	Qwen2.5-32B-VL	93.09	91.30	90.02	94.62	94.37		Qwen2.5-32B-VL	95.07	4.47	94.92	0.00	96.13
Qwen3-8B	91.72	91.38	91.04	44.11	71.50	Qwen3-8B	93.56	39.58	30.71	17.97	94.77		

Dataset	Model	Pure Instr.+		Pure Image	OCR-1P	OCR-2P
		Text	Image			
		(T)	(T+I)	(I)	(T→I)	(I→T)
GPQA	GPT-5.2	81.25	81.25	80.13	77.90	80.58
	InternVL3-8B	33.71	32.14	32.81	30.58	33.26
	InternVL3.5-8B	42.63	40.40	34.60	40.18	46.21
	Pixtral-12B	31.25	30.36	27.23	29.69	30.36
	Qwen2.5-7B-VL	34.15	34.15	30.58	27.90	32.59
	Qwen2.5-32B-VL	42.41	41.52	43.97	43.08	43.30
Qwen3-8B	43.75	39.29	35.04	37.28	36.38	

**Table 1:** Performance of different input modalities on four synthetic-image datasets (MMLU, ARC, HumanEval, GSM8K) and the graduate-level science benchmark GPQA. Cell shading indicates the performance difference relative to **Pure Text**: **red** indicates the modality outperforms text, **blue** indicates it underperforms text, and stronger shading reflects larger gaps.

reveals the largest modality gaps overall, with drops exceeding 60 points for several models.

*Performance on natural images.* Tab. 2 reports results on QASPER and SQuAD, where image inputs come from naturally occurring documents rather than synthetic renderings. On QASPER, the trend reverses: almost all models experience a performance gain when switching from text to image. These gains likely reflect the alignment between real PDF images and the document-heavy pretraining data of modern MLLMs. On SQuAD, the behavior is more model-dependent: Qwen2.5-VL-7B benefits from images, whereas GPT-5.2 sees a much larger drop. As a sanity check, converting QASPER and SQuAD into synthetic renderings yields lower accuracy than natural images (Tab. S2), confirming that the gains are from the realistic visual distribution rather than the image modality per se.

*Divergent robustness across models.* As shown by the cell shading in Tab. 1 and Tab. 2, MLLMs exhibit sharply different responses to modality changes. InternVL3.5-8B is the most modality-robust model, maintaining near-zero or positive differences on nearly all benchmarks. Qwen2.5-VL-7B also shows strong robustness, with image often being its better-performing modality. These discrepancies may stem from differences in vision encoder capability; we therefore use the OCR-1P and OCR-2P settings to measure recognition quality directly.

## 4.2 Image Recognition Cannot Fully Explain the Modality Gap

The two OCR settings in Tab. 1 reveal an asymmetric pattern across tasks. OCR-1P catastrophically fails for most models on many datasets. This suggests

Dataset	Model	Pure Text	Instr.+Image	Pure Image	OCR-2P	OCR-1P
		(P)	(P+I)	(I)	(I→P)	(I)
QASPER	GPT-5.2	51.92	75.10	77.25	-	74.27
	Qwen2.5-7B-VL	30.49	66.32	64.38	-	57.05
	Qwen3-8B-VL	53.27	76.25	70.75	-	56.89
	InternVL3-8B	44.02	69.36	54.43	-	56.15
	InternVL3.5-8B	49.38	57.66	61.07	-	55.68
SQuAD v2	GPT-5.2	97.50	85.50	71.69	67.11	84.74
	Qwen2.5-7B-VL	80.00	82.50	83.50	81.50	77.00
	Qwen3-8B-VL	95.00	85.50	85.50	84.00	84.50
	InternVL3-8B	82.50	84.00	76.50	73.50	69.50
	InternVL3.5-8B	98.00	83.50	86.00	79.50	84.00
	Pixtral-12B	91.50	81.00	83.50	82.50	84.50

**Table 2:** Performance of different input modalities on two real-image datasets QASPER and SQuAD v2. Cell shading indicates the performance difference relative to Pure Text: **red** indicates the modality outperforms text, **blue** indicates it underperforms text. Image-based inputs such as Pure Image and Instr.+Image outperform Pure Text on QASPER, indicating that MLLMs can benefit from naturally occurring visual text.<sup>7</sup>

that single-pass OCR-then-reason is not a natural operation mode for current MLLMs, and that solving the Pure Image task differs from solving the OCR-1P setting. In contrast, OCR-2P recovers a portion of the performance: InternVL3-8B increases from 42.53 to 87.87 on GSM8K when switching from Pure Image to OCR-2P, and Pixtral-12B sees a 42-point improvement. However, OCR-2P destroys code generation in many models: multiple models score zero on HumanEval with OCR-2P, suggesting that OCR strips structural cues such as indentation, alignment, and whitespace that are critical for code comprehension. To quantify this relationship, we compute the correlation between OCR-2P word error rate and Pure Image accuracy across all models and tasks, obtaining only 0.238. This suggests that overall OCR quality is a poor predictor of image-mode performance; errors on a small number of task-critical tokens (e.g., operators, variable names) may matter more than aggregate recognition accuracy.

### 4.3 Rendering Choices Confound Visual Evaluation

The results above show that MLLMs often suffer substantial drops when text is replaced with synthetic renderings, yet perform well on natural document images. We hypothesize that this discrepancy arises from a distributional mismatch between evaluation images and the text images encountered during pretraining, and investigate two rendering dimensions: typeface and color scheme, and image resolution.

*Visual format ablations.* We create four visual variants of the same underlying text: a default rendering using

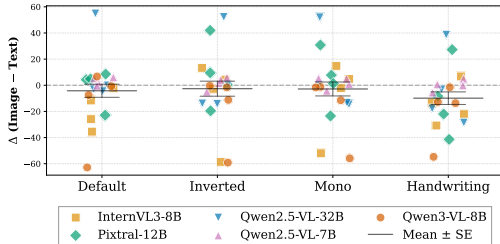


**Fig. 3:** Performance difference between Pure Text and Pure Image with different renderings. Each point is a dataset-model pair. Handwriting consistently causes larger negative drops than all the other settings.

black text on a white background in `NotoSansMath`; an inverted version with white text on a black background; a monospaced version rendered in `DejaVuSans Mono`, resembling terminal output; and a handwriting-style version rendered with `Priestacy`, introducing a large allographic shift unlikely to appear in standard pretraining corpora. Figure 3 presents the results.

Inverted and monospaced renderings perform similarly to the default, while the handwriting-style rendering produces the largest degradation across all models. Since all variants contain identical semantic content, font choice is an important confounding factor in visual text evaluation, contrary to [35], who find font has no effect on cross-modal consistency. This pattern supports the hypothesis that the modality gap is partly a training-distribution artifact: styles common in pretraining data (inverted, monospaced) cause minimal harm, whereas the handwriting font, which is rarely present in standard corpora, leads to the steepest drop.

#### *Image resolution and compression.*

Representing text as images can yield higher information density per token [24], but the computational cost depends on resolution, and higher resolution may not always help if it exceeds the model’s visual processing capacity. We conduct two complementary experiments: (a) resolution rescaling, where the input image is re-rendered at fractional resolutions ( $0.25\times$ ,  $0.5\times$ ,  $0.75\times$ ,  $1.0\times$ ) of the original dimensions, and (b) a compact rendering setup (10pt), where text is re-rendered at a 10-point font size with anti-aliasing on the original full-resolution canvas, concentrating all content into a small text bounding box that occupies only 5–11% of the total pixel area.

Figure 4 presents accuracy as a function of resolution scale on HumanEval and ARC. Most models exhibit a resolution threshold: performance remains high at  $0.50\times$ – $1.0\times$  but drops sharply at lower resolutions. InternVL3.5, the only model with a Visual Resolution Router (ViR) [39], is remarkably resolution-invariant, with no performance decrease at  $0.25\times$ . Even at 25% of the original resolution, image mode consumes more FLOPs than text mode (Table S3), suggesting that compute efficiency is not guaranteed without specialized optimiza-

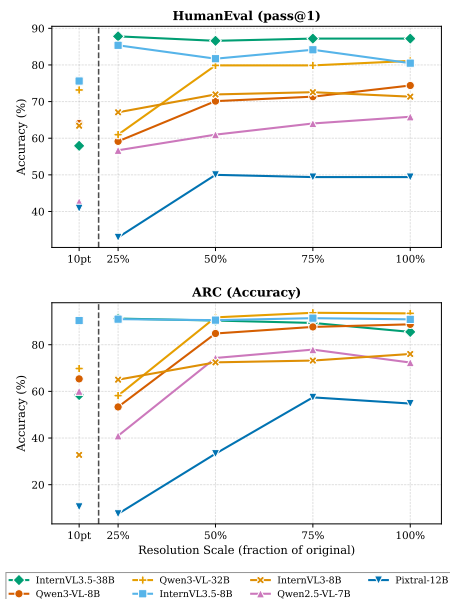


**Fig. 4:** The performance with respect to the image resolution scale on HumanEval (top) and ARC (bottom). The black vertical dashed line indicates the point where the **Pure Image** consumes the same FLOPs as the **Pure Text** mode. Most models remain a stable performance until the resolution reaches a certain lower bound, while InternVL-3.5-8B maintains stable performance across all resolutions.

tion. The 10pt setup offers a promising alternative: all models achieve higher performance with 10pt than with their higher-resolution counterparts, indicating that smart compression that preserves critical visual features can mitigate resolution sensitivity. Overall, these rendering experiments show that font, color, and resolution are strong confounders, and benchmarks should report rendering specifications when evaluating visual text reasoning.

## 5 Error Analysis

The aggregate performance numbers in Section 4 show that image mode degrades accuracy, but not *why*. To move beyond surface-level accuracy comparisons, we conduct a systematic error analysis following *grounded theory* [14], a qualitative research method that constructs a taxonomy directly from observational data. We classify over 4,000 individual errors across all models and five datasets under three input modes (`Pure Text`, `Pure Image`, `Instr.+Image`).

### 5.1 Method

Grounded theory is an inductive qualitative research method that derives a theoretical framework directly from data rather than testing pre-existing hypotheses [14]. It proceeds through iterative coding phases: *open coding*, which segments raw observations into initial descriptive labels; *constant comparison*, which refines codes by classifying new data against existing categories; and *axial coding*, which groups related codes into higher-level categories and maps their relationships. Because the canonical process requires extensive manual effort, and recent studies have shown that LLM agents can effectively perform inductive coding [6, 38, 45], we adopt a human-in-the-loop variant: GPT-5.2 performs the open coding and constant comparison while human annotators review all proposed changes and conduct the final axial coding to ensure coherence and validity.

*Phase 1: Open coding.* We sample 1,000 errors uniformly across models, datasets, and modalities. For each error, the model receives the original input (question and answer choices where applicable), ground-truth answer, and the model’s raw response, and proposes a short failure description along with a candidate error label. The model maintains a running set of codes and can either assign an instance to an existing code or propose a new one. This phase produced 415 initial codes.

*Phase 2: Constant comparison.* New errors are randomly sampled and classified against existing codes. For each instance, the model determines whether the error matches an existing code, requires a new code, or warrants updating an existing description. A human annotator reviews every proposed new code, merge, or description update, approving or rejecting changes. Saturation is reached when no new codes are added for 50 consecutive instances. Codes occurring only once are pruned unless conceptually critical, and the corresponding errors are assigned to a miscellaneous category.

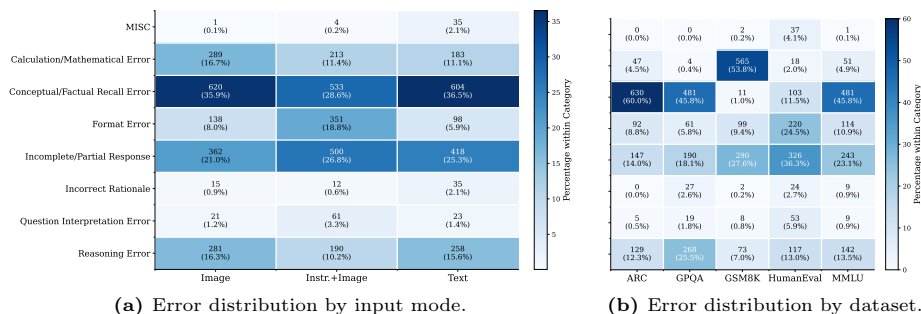


**Fig. 5:** Distribution of error categories across input modes (left) and datasets (right). Cell values show raw counts and within-column percentages.

*Phase 3: Axial coding.* A human researcher reviews all codes and groups them into organizing dimensions, producing the final taxonomy of primary error categories along with a miscellaneous category.

## 5.2 Error Taxonomy and Findings

The coding process above yields the following taxonomy. We then classify a larger sample of up to 150 errors per model–dataset pair, yielding 4,195 errors across 33 pairs. Each error is classified into one of these categories.

1. **Conceptual/Factual Recall Error (30.4%):** Confusion or misunderstanding of foundational concepts, factual inaccuracies, or domain knowledge misapplication.
2. **Incomplete/Partial Response (26.0%):** The model does not provide an answer in its response, or its output is truncated, empty, or incomplete.
3. **Calculation/Mathematical Error (16.2%):** Errors in arithmetic, computation, or numerical reasoning.
4. **Format/Output Error (12.5%):** Incorrect formatting, failure to follow output structure instructions (e.g., missing answer tags).
5. **Reasoning Error (11.0%):** Incorrect logic, flawed inference, or faulty causal reasoning.
6. **Question Interpretation Error (2.1%):** Misreading, misunderstanding, or misinterpreting the intent or phrasing of the question.
7. **Incorrect Rationale (0.8%):** The model selects the correct answer but provides a contradictory or unsupported explanation.

*Image mode increases reading errors but not knowledge or reasoning errors.* Comparing the error distributions between image mode and text mode in Figure 5a, we observe a clear asymmetry. *Calculation errors* increase by 1.5 $\times$  under image input (16.7% vs. 11.1%), and *format errors* rise from 5.9% to 8.0%. These categories stem from misreading the input: misperceiving digits or operators

from rendered text, or failing to follow output formatting instructions. In contrast, *conceptual/factual recall errors*, which require retrieving domain knowledge rather than reading the input, remain virtually unchanged, and *reasoning errors* show only a modest increase. This pattern indicates that image mode primarily impairs the model’s ability to accurately extract text-level information from pixels, while knowledge retrieval and logical inference remain largely unaffected.

*Dataset-specific error profiles.* The error distribution varies substantially across tasks (Figure 5b), reflecting their different requirements. GSM8K errors are dominated by calculation failures, consistent with the observation that misread digits cascade into incorrect arithmetic. ARC, GPQA, and MMLU are dominated by conceptual/factual recall errors (60.0%, 45.8%, and 45.8%, respectively), reflecting the knowledge-intensive nature of these benchmarks; GPQA additionally shows the highest reasoning error rate (25.5%), consistent with the difficulty of graduate-level science questions. HumanEval exhibits a distinct profile: incomplete/partial responses account for 36.3% of errors and format errors for 24.5%, suggesting that code generation is particularly sensitive to output formatting under visual input.

*Chain-of-thought reasoning collapse.* Beyond error categories, we observe that some models produce substantially shorter responses and are much less likely to output chain-of-thought (CoT) reasoning on GSM8K in image mode. Qwen3-VL-8B shows this most prominently, averaging 618 characters in text mode but only 32 in image mode (19× reduction); Pixtral averages 115 characters in text mode but only 23 in image mode (5× reduction). In these instances, the model largely forgoes step-by-step reasoning, jumping directly to often incorrect answers instead of producing the intermediate computation that text mode elicits. This reasoning collapse contributes to the high calculation error rate on GSM8K: without explicit CoT, arithmetic mistakes go undetected and uncorrected.

These findings show that the modality gap is driven by two complementary mechanisms: difficulty in accurately reading text from pixels, and image mode suppressing the model’s propensity to engage in chain-of-thought reasoning. Motivated by these observations, in Section 6 we distill the model’s own text-mode reasoning traces into its visual pathway, targeting both the reading deficit and the reasoning collapse.

## 6 Bridging the Modality Gap via Self-Distillation

Our error analysis (Section 5) traced the modality gap to two mechanisms: difficulty reading text from pixels and a collapse in chain-of-thought reasoning. To address both, we propose *self-distillation*: the model’s own text-mode reasoning supervises its visual pathway, teaching it to reproduce the same multi-step reasoning from rendered images.

Strategy	Benchmark	Baseline		Self-Distilled		$ \Delta(\text{Text} - \text{Image}) $
		Text (  )	Image (  )	Text (  )	Image (  )	
ViT+LM (unfiltered)	GSM8K	93.56	30.71	93.71	91.28	2.43
ViT+LM (filtered)		93.56	30.71	93.30	92.57	0.73
ViT-only		93.56	30.71	93.25	85.29	7.96
LM-only				<b>94.09</b>	<b>92.72</b>	1.37
	GSM8K	93.56	30.71	<b>94.09</b>	<b>92.72</b>	62.85→1.37
LM-only	ARC	91.72	91.04	91.47	91.89	0.68→0.42
	MMLU	78.44	71.01	75.49	72.70	7.43→2.79
	HumanEval	76.22	82.93	84.15	82.32	6.71→1.83

**Table 3:** Self-distillation results on Qwen3-VL-8B. *Above the dashed line:* freezing ablation on GSM8K. LM-only training preserves text-mode accuracy while recovering image-mode performance; ViT-only training improves image-mode accuracy but leaves a larger residual gap. *Below:* the GSM8K-trained LM-only model evaluated on other benchmarks to test for catastrophic forgetting.  $|\Delta|$  denotes the absolute text-image accuracy gap; arrows show the reduction from baseline to self-distilled.

## 6.1 Experimental Setup

We select GSM8K because it exhibits one of the largest modality gaps and provides a standard training split. We run Qwen3-VL-8B in **Pure Text** mode on GSM8K and collect its CoT traces as supervised targets, each paired with the corresponding **Pure Image** input. To prevent text-mode performance from degrading, we include the original text-mode training data alongside the image-mode distillation targets. All experiments use LoRA [22] with rank  $r=64$ , trained for 2 epochs with a learning rate of  $2 \times 10^{-4}$  and an effective batch size of 16. Unlike standard distillation, which transfers soft labels, our setting requires transferring multi-step reasoning traces. Gold reasoning traces are unavailable, and ground-truth answers alone are insufficient since they lack the intermediate steps that guide the model’s generation. We therefore use the model’s own text-mode CoT outputs as supervision. Because some traces lead to incorrect answers, we compare two variants: **filtered** (retaining only traces with correct final answers) and **unfiltered** (using all traces regardless of correctness). Using filtered traces, we also compare three fine-tuning strategies: (1) **ViT+LM**, applying LoRA to both the vision encoder and the language model; (2) **LM-only**, freezing the vision encoder; and (3) **ViT-only**, freezing the language model.

## 6.2 Results

*Unfiltered traces suffice.* To test whether correctness of the teacher signal matters, we compare training on filtered traces (only those leading to correct answers) against all raw CoT traces. As shown in Table 3, filtered and unfiltered traces achieve 92.57% and 91.28% image-mode accuracy, respectively, a gap of only 1.29%. Since the model already achieves 93.56% accuracy in text mode, the vast majority of traces are high-quality reasoning demonstrations. The small proportion of incorrect traces do not meaningfully degrade training, suggesting

that the reasoning *structure* of the supervision signal matters more than perfect correctness. Text-mode accuracy is preserved in both variants because the original text-mode training data is included alongside the distillation targets.

*Adapting the language model is critical.* Among the three fine-tuning strategies, all substantially close the modality gap, but to different degrees. ViT-only training already raises image-mode accuracy from 30.71% to 85.29%, showing that better visual feature alignment alone yields substantial gains. LM-only and ViT+LM training achieve comparable results (92.72% and 92.57%, respectively), both reducing the text-image gap to under 1.4% (Table 3), indicating that adapting the language model is the key factor and adding ViT adaptation provides little additional benefit. One possible explanation for the asymmetry between ViT-only and LM-only lies in capacity: the vision encoder has roughly 0.4B parameters versus 8B in the language model, so LoRA applied to the larger module can absorb more of the distillation signal.

*No catastrophic forgetting.* We evaluate the GSM8K-trained LM-only model on ARC, MMLU, and HumanEval to test whether single-benchmark distillation degrades general capabilities. As shown in Table 3 (below the dashed line), the model preserves, and in some cases improves, performance across all benchmarks, with the text-image gap narrowing on every task. This confirms that the self-distillation signal transfers general visual-text alignment rather than task-specific shortcuts.

## 7 Conclusion

We move beyond reporting the text-vs-image accuracy gap to diagnosing why it arises and how it can be closed. Across seven benchmarks, seven models, and five input modes, we find that MLLMs already perform strongly on natural document images, while struggling primarily on synthetic renderings whose visual properties diverge from pretraining distributions. Rendering choices such as font, resolution, and compression are critical confounds that can shift accuracy by tens of percentage points, and should be reported alongside model results. An error taxonomy built from over 4,000 failures shows that image mode selectively amplifies perceptual errors while leaving cognitive errors largely unchanged: image mode impairs reading, not thinking. We also observe a chain-of-thought reasoning collapse, where models produce dramatically shorter outputs under visual input, bypassing step-by-step reasoning. Finally, self-distillation experiments show that training the model on its own text-mode reasoning traces paired with image inputs substantially narrows the gap, with both vision encoder and language model adaptation contributing. Together, our results suggest that the reported gaps stem largely from rendering artifacts and a misalignment between visual features and the model’s reasoning capabilities, pointing to a more optimistic outlook for pixel-based language understanding.

## References

- [1] Agrawal, P., Antoniak, S., Hanna, E.B., Bout, B., Chaplot, D., Chudnovsky, J., Costa, D., De Monicault, B., Garg, S., Gervet, T., et al.: Pixtral 12b. arXiv preprint arXiv:2410.07073 (2024) [1](#)
- [2] Agrawal, P., Antoniak, S., Hanna, E.B., Bout, B., Chaplot, D., Chudnovsky, J., Costa, D., Monicault, B.D., Garg, S., Gervet, T., Ghosh, S., Héliou, A., Jacob, P., Jiang, A.Q., Khandelwal, K., Lacroix, T., Lample, G., Casas, D.L., Lavril, T., Scao, T.L., Lo, A., Marshall, W., Martin, L., Mensch, A., Muddireddy, P., Nemychnikova, V., Pellat, M., Platen, P.V., Raghuraman, N., Rozière, B., Sablayrolles, A., Saulnier, L., Sauvestre, R., Shang, W., Soletskyi, R., Stewart, L., Stock, P., Studnia, J., Subramanian, S., Vaze, S., Wang, T., Yang, S.: Pixtral 12b (2024), <https://arxiv.org/abs/2410.07073> [6](#)
- [3] Bai, J., Bai, S., Yang, S., Wang, S., Tan, S., Wang, P., Lin, J., Zhou, C., Zhou, J.: Qwen-vl: A versatile vision-language model for understanding, localization, text reading, and beyond (2023), <https://arxiv.org/abs/2308.12966> [1](#)
- [4] Bai, S., Chen, K., Liu, X., Wang, J., Ge, W., Song, S., Dang, K., Wang, P., Wang, S., Tang, J., Zhong, H., Zhu, Y., Yang, M., Li, Z., Wan, J., Wang, P., Ding, W., Fu, Z., Xu, Y., Ye, J., Zhang, X., Xie, T., Cheng, Z., Zhang, H., Yang, Z., Xu, H., Lin, J.: Qwen2.5-vl technical report (2025), <https://arxiv.org/abs/2502.13923> [6](#)
- [5] Biten, A.F., Tito, R., Mafla, A., Gomez, L., Rusiñol, M., Valveny, E., Jawahar, C.V., Karatzas, D.: Scene text visual question answering (2019), <https://arxiv.org/abs/1905.13648> [4](#)
- [6] Cemri, M., Pan, M.Z., Yang, S., Agrawal, L.A., Chopra, B., Tiwari, R., Keutzer, K., Parameswaran, A., Klein, D., Ramchandran, K., Zaharia, M., Gonzalez, J.E., Stoica, I.: Why do multi-agent llm systems fail? (2025), <https://arxiv.org/abs/2503.13657> [10](#)
- [7] Chen, M., Tworek, J., Jun, H., Yuan, Q., de Oliveira Pinto, H.P., Kaplan, J., Edwards, H., Burda, Y., Joseph, N., Brockman, G., Ray, A., Puri, R., Krueger, G., Petrov, M., Khlaaf, H., Sastry, G., Mishkin, P., Chan, B., Gray, S., Ryder, N., Pavlov, M., Power, A., Kaiser, L., Bavarian, M., Winter, C., Tillet, P., Such, F.P., Cummings, D., Plappert, M., Chantzis, F., Barnes, E., Herbert-Voss, A., Guss, W.H., Nichol, A., Paino, A., Tezak, N., Tang, J., Babuschkin, I., Balaji, S., Jain, S., Saunders, W., Hesse, C., Carr, A.N., Leike, J., Achiam, J., Misra, V., Morikawa, E., Radford, A., Knight, M., Brundage, M., Murati, M., Mayer, K., Welinder, P., McGrew, B., Amodei, D., McCandlish, S., Sutskever, I., Zaremba, W.: Evaluating large language models trained on code (2021) [5](#), [2](#)
- [8] Chen, Z., Wang, W., Cao, Y., Liu, Y., Gao, Z., Cui, E., Zhu, J., Ye, S., Tian, H., Liu, Z., et al.: Expanding performance boundaries of open-source multimodal models with model, data, and test-time scaling. arXiv preprint arXiv:2412.05271 (2024) [6](#)

- [9] Chen, Z., Wu, J., Wang, W., Su, W., Chen, G., Xing, S., Zhong, M., Zhang, Q., Zhu, X., Lu, L., et al.: Internvl: Scaling up vision foundation models and aligning for generic visual-linguistic tasks. In: Proceedings of the IEEE/CVF Conference on Computer Vision and Pattern Recognition. pp. 24185–24198 (2024) [1](#)
- [10] Cheng, J., Liu, Y., Zhang, X., Fei, Y., Hong, W., Lyu, R., Wang, W., Su, Z., Gu, X., Liu, X., et al.: Glyph: Scaling context windows via visual-text compression. arXiv preprint arXiv:2510.17800 (2025) [2](#), [3](#)
- [11] Clark, P., Cowhey, I., Etzioni, O., Khot, T., Sabharwal, A., Schoenick, C., Tafjord, O.: Think you have solved question answering? try arc, the ai2 reasoning challenge. arXiv:1803.05457v1 (2018) [5](#)
- [12] Clavié, B., Brand, F.: Readbench: Measuring the dense text visual reading ability of vision-language models (2025), <https://arxiv.org/abs/2505.19091> [5](#)
- [13] Cobbe, K., Kosaraju, V., Bavarian, M., Chen, M., Jun, H., Kaiser, L., Plappert, M., Tworek, J., Hilton, J., Nakano, R., Hesse, C., Schulman, J.: Training verifiers to solve math word problems. arXiv preprint arXiv:2110.14168 (2021) [5](#)
- [14] Corbin, J., Strauss, A.: Basics of qualitative research: Techniques and procedures for developing grounded theory. Sage publications (2014) [10](#)
- [15] Dasigi, P., Lo, K., Beltagy, I., Cohan, A., Smith, N.A., Gardner, M.: A dataset of information-seeking questions and answers anchored in research papers (2021) [4](#), [5](#), [1](#)
- [16] Dehaene, S., Cohen, L.: Cultural recycling of cortical maps. *Neuron* **56**(2), 384–398 (2007) [1](#)
- [17] Dehaene-Lambertz, G., Monzalvo, K., Dehaene, S.: The emergence of the visual word form: Longitudinal evolution of category-specific ventral visual areas during reading acquisition. *PLoS biology* **16**(3), e2004103 (2018) [1](#)
- [18] Gao, T., Wang, Z., Bhaskar, A., Chen, D.: Improving language understanding from screenshots (2024), <https://arxiv.org/abs/2402.14073> [2](#), [3](#)
- [19] Gupta, S., Hoffman, J., Malik, J.: Cross modal distillation for supervision transfer (2015), <https://arxiv.org/abs/1507.00448> [4](#)
- [20] Hendrycks, D., Burns, C., Basart, S., Critch, A., Li, J., Song, D., Steinhardt, J.: Aligning ai with shared human values. Proceedings of the International Conference on Learning Representations (ICLR) (2021) [5](#)
- [21] Hendrycks, D., Burns, C., Basart, S., Zou, A., Mazeika, M., Song, D., Steinhardt, J.: Measuring massive multitask language understanding. Proceedings of the International Conference on Learning Representations (ICLR) (2021) [5](#)
- [22] Hu, E.J., Shen, Y., Wallis, P., Allen-Zhu, Z., Li, Y., Wang, S., Wang, L., Chen, W.: LoRA: Low-rank adaptation of large language models. In: International Conference on Learning Representations (2022) [13](#)
- [23] Hu, K., Cy, A., Qiu, L., Ding, X.D., Wang, R., Zhu, Y.E., Andreas, J., He, K.: Arc is a vision problem! arXiv preprint arXiv:2511.14761 (2025) [4](#)
- [24] Li, Y., Lan, Z., Zhou, J.: Text or pixels? evaluating efficiency and understanding of LLMs with visual text inputs. In: Christodoulopoulos, C.,

- Chakraborty, T., Rose, C., Peng, V. (eds.) Findings of the Association for Computational Linguistics: EMNLP 2025. pp. 10564–10578. Association for Computational Linguistics, Suzhou, China (Nov 2025). <https://doi.org/10.18653/v1/2025.findings-emnlp.558>, <https://aclanthology.org/2025.findings-emnlp.558/> 4, 9
- [25] Liu, H., Li, C., Wu, Q., Lee, Y.J.: Visual instruction tuning (2023) 1
- [26] Liu, Q., Feng, J., Wang, Y., Han, X., Cheng, Y., Zhu, Y., Diao, H., Zhuge, Y., Lu, H.: Vista-bench: Do vision-language models really understand visualized text as well as pure text? arXiv preprint arXiv:2602.04802 (2026) 4
- [27] Lyu, Z., Ma, X., Chen, W.: Pixelworld: How far are we from perceiving everything as pixels? (2025), <https://arxiv.org/abs/2501.19339> 2, 4, 5
- [28] Pham, T., Nguyen, N., Zunjare, P., Chen, W., Tseng, Y.M., Vu, T.: Sealqa: Raising the bar for reasoning in search-augmented language models (2025), <https://arxiv.org/abs/2506.01062> 5, 1
- [29] Rajpurkar, P., Jia, R., Liang, P.: Know what you don't know: Unanswerable questions for SQuAD. In: Gurevych, I., Miyao, Y. (eds.) Proceedings of the 56th Annual Meeting of the Association for Computational Linguistics (Volume 2: Short Papers). pp. 784–789. Association for Computational Linguistics, Melbourne, Australia (Jul 2018). <https://doi.org/10.18653/v1/P18-2124>, <https://aclanthology.org/P18-2124> 5
- [30] Rajpurkar, P., Zhang, J., Lopyrev, K., Liang, P.: SQuAD: 100,000+ questions for machine comprehension of text. In: Su, J., Duh, K., Carreras, X. (eds.) Proceedings of the 2016 Conference on Empirical Methods in Natural Language Processing. pp. 2383–2392. Association for Computational Linguistics, Austin, Texas (Nov 2016). <https://doi.org/10.18653/v1/D16-1264>, <https://aclanthology.org/D16-1264> 4
- [31] Rein, D., Hou, B.L., Stickland, A.C., Petty, J., Pang, R.Y., Dirani, J., Michael, J., Bowman, S.R.: GPQA: A graduate-level google-proof q&a benchmark. arXiv preprint arXiv:2311.12022 (2023) 5, 2
- [32] Rust, P., Lotz, J.F., Bugliarello, E., Salesky, E., de Lhoneux, M., Elliott, D.: Language modelling with pixels. arXiv preprint arXiv:2207.06991 (2022) 2, 3
- [33] Sidorov, O., Hu, R., Rohrbach, M., Singh, A.: Textcaps: a dataset for image captioning with reading comprehension (2020), <https://arxiv.org/abs/2003.12462> 4
- [34] Singh, A., Natarajan, V., Shah, M., Jiang, Y., Chen, X., Batra, D., Parikh, D., Rohrbach, M.: Towards vqa models that can read (2019), <https://arxiv.org/abs/1904.08920> 4
- [35] van Sprang, A., Samson, L., Lucic, A., Acar, E., Ghebreab, S., Asano, Y.M.: Same content, different answers: Cross-modal inconsistency in mllms. arXiv preprint arXiv:2512.08923 (2025) 2, 4, 9
- [36] Team, G., Kamath, A., Ferret, J., Pathak, S., Vieillard, N., Merhej, R., Perrin, S., Matejovicova, T., Ramé, A., Rivière, M., et al.: Gemma 3 technical report. arXiv preprint arXiv:2503.19786 (2025) 1

- [37] Tian, Y., Krishnan, D., Isola, P.: Contrastive representation distillation (2022), <https://arxiv.org/abs/1910.10699> 4
- [38] Wan, R., Wang, H., Huang, T.H., Gao, J.: From noise to nuance: Enriching subjective data annotation through qualitative analysis. In: Proceedings of the Fourth Workshop on Bridging Human-Computer Interaction and Natural Language Processing (HCI+ NLP). pp. 240–254 (2025) 10
- [39] Wang, W., Gao, Z., Gu, L., Pu, H., Cui, L., Wei, X., Liu, Z., Jing, L., Ye, S., Shao, J., et al.: Internvl3. 5: Advancing open-source multimodal models in versatility, reasoning, and efficiency. arXiv preprint arXiv:2508.18265 (2025) 6, 9
- [40] Wang, X., Cui, Y., Wang, J., Zhang, F., Wang, Y., Zhang, X., Luo, Z., Sun, Q., Li, Z., Wang, Y., et al.: Multimodal learning with next-token prediction for large multimodal models. Nature pp. 1–7 (2026) 2, 3
- [41] Wang, Z., Wang, Y., Cai, Y.: Cure or poison? embedding instructions visually alters hallucination in vision-language models. arXiv preprint arXiv:2508.01678 (2025) 4
- [42] Wei, J., Sun, Z., Papay, S., McKinney, S., Han, J., Fulford, I., Chung, H.W., Passos, A.T., Fedus, W., Glaese, A.: Browsecomp: A simple yet challenging benchmark for browsing agents (2025), <https://arxiv.org/abs/2504.12516> 5, 1
- [43] Xing, L., Wang, A.J., Yan, R., Qu, H., Li, Z., Tang, J.: See the text: From tokenization to visual reading. arXiv preprint arXiv:2510.18840 (2025) 2, 3
- [44] Yang, A., Li, A., Yang, B., Zhang, B., Hui, B., Zheng, B., Yu, B., Gao, C., Huang, C., Lv, C., et al.: Qwen3 technical report. arXiv preprint arXiv:2505.09388 (2025) 6
- [45] Zhong, M., Wang, P., Field, A.: Hicode: Hierarchical inductive coding with llms. In: Proceedings of the 2025 Conference on Empirical Methods in Natural Language Processing. pp. 31048–31066 (2025) 10

## A Realistic Data Preparation

**QASPER** [15] is a long-form QA dataset over scientific articles that often requires multi-sentence reasoning. All instances that require access to tables and figures are removed to ensure a fair comparison between the **Pure Text** format and **Pure Image** format. We download the original PDF files from arXiv and convert all pages into PNG images using the *fitz* library, excluding the reference section, which is also not included in the **Pure Text** format of QASPER. For each example in **SQuAD** v2, we capture a screenshot of the corresponding Wikipedia page to create a natural-image version of the context. The corresponding screenshot is manually aligned with the passages given in the original SQuAD v2 data. Due to the nature of webpages, there would be unavoidable truncations of images or tables in the **Pure Image** input that is not included by the **Pure Text** setting. For evaluation, zero-shot inference on QA tasks does not align well with the original span-based metrics, because MLLMs are not trained to reproduce annotation artifacts such as exact spans. Instead, following recent information-seeking benchmarks [28, 42], we adopt an LLM-as-judge protocol, where we use GPT-5 (*gpt-5-2025-08-07*) to compare the model prediction with the gold answer and report accuracy over all examples. Results on span-based metrics can be found in Section F.

## B Detailed Input Settings

This section provides the full input formats used across all configurations, along with examples for each dataset. Unless otherwise specified, models are prompted to produce outputs wrapped in `<answer>...</answer>`. For datasets that require structured or non-free-form outputs, we apply a permissive parsing strategy to extract the final predictions. All evaluations are conducted in a zero-shot setting. Accuracy is used as the primary metric for all benchmarks, with the exception of HumanEval, which is evaluated using `pass@k`, where  $k = 1$ .

*MMLU* MMLU evaluates a model’s knowledge and reasoning ability across 57 subjects spanning the humanities, social sciences, STEM fields, and professional domains. Each question is multiple-choice and often requires domain-specific expertise. In our setting, we adopt its original tasks and targets. The example input for MMLU is shown in Figure S1.

*ARC* ARC-Challenge (ARC) assesses a model’s ability to perform complex, non-trivial reasoning on grade-school science questions. Unlike its easier counterpart (ARC-Easy), ARC is intentionally adversarial: questions cannot be solved by surface heuristics and typically require multi-step inference, commonsense knowledge, or integration of scientific facts. We adopt its original tasks and targets, and the example input for ARC-C is shown in Figure S2.

Most rocks on the Moon's surface are older than those on the Earth's surface. The best evidence for this is: Enclose only the final answer within <answer> and </answer>. Do not include any additional text inside the tags.

- A. Lunar rocks are composed of fragments pulverized by many impacts.
- B. Radioactive dating of lunar samples shows that they are older.
- C. The Moon's surface is more heavily eroded than the Earth's surface.
- D. The Moon's surface has more impact craters than the Earth's surface.

(a) Image format.

Text	<p>Answer the following multiple choice question. Respond with just the letter of the correct answer (A, B, C, or D).          Most rocks on the Moon's surface are older than those on the Earth's surface. The best evidence for this is:          A. Lunar rocks are composed of fragments pulverized by many impacts.          B. Radioactive dating of lunar samples shows that they are older.          C. The Moon's surface is more heavily eroded than the Earth's surface.          D. The Moon's surface has more impact craters than the Earth's surface.          Enclose only the final answer within &lt;answer&gt; and &lt;/answer&gt;. Do not include any additional text inside the tags.</p>
Instr. + Image	<p>Please follow the instruction in the image. Enclose only the final answer within &lt;answer&gt; and &lt;/answer&gt;. Do not include any additional text inside the tags. [Image provided in (a) without the format instructions.]</p>

(b) Text and Instr. + Image format.

**Fig. S1:** An example input of MMLU.

*GPQA* GPQA [31] is a graduate-level question answering benchmark consisting of 448 challenging multiple-choice questions in physics, chemistry, and biology. The questions are crafted by domain experts and are designed to be difficult even for specialists outside their own subfield, requiring deep domain knowledge and multi-step scientific reasoning. We adopt its original tasks and targets, and the example input for GPQA is shown in Figure S3.

*HumanEval* HumanEval [7] measures a model's ability to synthesize correct and executable code from natural language descriptions. Each task provides a short docstring specifying a function's intended behavior, and models must generate a complete Python implementation that passes hidden unit tests. The example input of HumanEval is shown in Figure S4.

*GSM8K* GSM8K evaluates a model's ability to solve grade-school mathematical word problems that require multi-step reasoning. Each question is free-form and demands 2 to 8 steps to arrive at the final answer. The solution of GSM8K is provided in natural language format, and a final answer is given after the reasoning steps. In our setting, we adopt its original data and consider primarily the correctness of the answer (extracting the answer from the reasoning chain). The example input for GSM8K is shown in Figure S5. To avoid confounding

Devil facial tumor disease (DFTD) is a disease that is decimating the population of Tasmanian devils. The disease passes from one animal to another through bites and is caused by parasites. The parasites cause cancerous tumors that spread throughout an infected animal's body and kill it. What is the best description of DFTD? Enclose only the final answer within <answer> and </answer>. Do not include any additional text inside the tags.

- A. a non-infectious, cell-cycle disease
- B. an infectious, cell-cycle disease
- C. a non-infectious, chronic disease
- D. an infectious, chronic disease

(a) Image format.

Text	<p>Answer the following multiple choice question. Respond with just the letter of the correct answer (A, B, C, or D).</p> <p>Devil facial tumor disease (DFTD) is a disease that is decimating the population of Tasmanian devils. The disease passes from one animal to another through bites and is caused by parasites. The parasites cause cancerous tumors that spread throughout an infected animal's body and kill it. What is the best description of DFTD?</p> <p>A. a non-infectious, cell-cycle disease", "an infectious, cell-cycle disease          B. an infectious, cell-cycle disease          C. a non-infectious, chronic disease          D. an infectious, chronic disease</p> <p>Enclose only the final answer within &lt;answer&gt; and &lt;/answer&gt;. Do not include any additional text inside the tags.</p>
Instr. + Image	<p>Please follow the instruction in the image. Enclose only the final answer within &lt;answer&gt; and &lt;/answer&gt;. Do not include any additional text inside the tags. [Image provided in (a) without the format instructions.]</p>

(b) Text and Instr. + Image format.

**Fig. S2:** An example input of ARC.

factors introduced by in-context examples, all the experiments are run on the zero-shot condition.

*SQuAD v2*. SQuAD v2 is an extractive question answering dataset that tests a model's ability to extract the answers from a given passage and to recognize unanswerable queries. Each instance presents a question and a supporting passage from Wikipedia, and models must either extract a precise span or correctly abstain when the passage lacks sufficient information.

*QASPER*. QASPER is a long-context reading comprehension task that evaluates a model's ability to answer questions about academic research papers. Each question targets specific information regarding methods, findings, assumptions, or limitations of the paper, requiring models to reason over evidence within full-length scientific documents. We feed the entire paper on a given question as the input. The example input for QASPER is shown in Figure S7.

A large gene has dozens of exons, of which the central ones code for folded triple helical repeats that connect the cytoskeleton with sarcolemma and extracellular space. Each exon usually codes for one folded triple alpha helix. The most common mutations of the gene are central exon deletions that create out-of-frame peptides and progressive degenerative organ waste. A solution is to deliver a Morpholino that recognizes the 5' end of the out-of-frame exon in pre-mRNA. The molecule prevents binding of the spliceosome and creates exon skipping and in-frame joining. Several missing exons are well tolerated by an organism. Which structure below is not involved in the proposed therapy?  
 Enclose only the final answer within <answer> and </answer>. Do not include any additional text inside the tags.

- A. antisense
- B. polyA tail
- C. lariat
- D. R-loops

(a) Image format.

Text	<p>A large gene has dozens of exons, of which the central ones code for folded triple helical repeats that connect the cytoskeleton with sarcolemma and extracellular space. Each exon usually codes for one folded triple alpha helix. The most common mutations of the gene are central exon deletions that create out-of-frame peptides and progressive degenerative organ waste. A solution is to deliver a Morpholino that recognizes the 5' end of the out-of-frame exon in pre-mRNA. The molecule prevents binding of the spliceosome and creates exon skipping and in-frame joining. Several missing exons are well tolerated by an organism. Which structure below is not involved in the proposed therapy?          Enclose only the final answer within &lt;answer&gt; and &lt;/answer&gt;. Do not include any additional text inside the tags.</p> <p>A. antisense B. polyA tail C. lariat D. R-loops</p>
Instr. + Image	<p>Please follow the instruction in the image. Enclose only the final answer within &lt;answer&gt; and &lt;/answer&gt;. Do not include any additional text inside the tags. [Image provided in (a) without the format instructions.]</p>

(b) Text and Instr. + Image format.

**Fig. S3:** An example input of GPQA.

## B.1 OCR Prompt

The prompt used in OCR-P2 is shown in Figure S8. It is also used in OCR-P1 as the guidelines for performing extractions.

## C Dataset Statistics

Table S1 summarizes the composition of our evaluation suite. The five synthetic-image benchmarks (MMLU, ARC, GPQA, GSM8K, and HumanEval) comprise 16,895 instances in total, with MMLU accounting for the largest share (83.0%). QASPER and SQuAD v2 use natural images and are listed separately.

## D Experiment Setting Details

We use a unified decoding setup across models and datasets. Unless otherwise noted, the temperature is set to 0.1 with a batch size of 8 and a maximum generation length of 1024 tokens. For code generation tasks, the temperature is set to 0.2 to ensure diversity on the generation results.

```

from typing import List

def separate_paren_groups(paren_string: str) -> List[str]:
    """ Input to this function is a string containing multiple groups of nested parentheses. Your goal is
    to
    separate those group into separate strings and return the list of those.
    Separate groups are balanced (each open brace is properly closed) and not nested within each
    other
    Ignore any spaces in the input string.
    >>> separate_paren_groups('() (()) (())')
    ['()', '(())', '(())']
    """

Complete the function above. Enclose only the complete function implementation within <answer>
and </answer>. Do not include any additional text inside the tags.

```

(a) Image format.

Text	<pre> from typing import List def separate_paren_groups(paren_string: str) -&gt; List[str]: """ Input to this function is a string containing multiple groups of nested parentheses. Your goal is to separate those group into separate strings and return the list of those. Separate groups are balanced (each open brace is properly closed) and not nested within each other Ignore any spaces in the input string. &gt;&gt; separate_paren_groups('() (()) (())') ['()', '(())', '(())'] """  Enclose only the final answer within &lt;answer&gt; and &lt;/answer&gt;. Do not include any additional text inside the tags. </pre>
Instr. + Image	<pre> Please follow the instruction in the image. Enclose only the final answer within &lt;answer&gt; and &lt;/answer&gt;. Do not include any additional text inside the tags. [Image provided in (a) without the format instructions.] </pre>

(b) Text and Instr. + Image format.

**Fig. S4:** An example input of HumanEval.

For OCR-1P, the maximum generation length is set to 4096, as the model is asked to perform OCR and solve the task in one inference. The generation length is increased to allow full inclusion of OCR results and task reasoning in one output.

## E Full Results Table

We report the complete performance of all models under all input configurations in Table S2. The table covers *PureText*, *PureImage*, *Inst.+Image* (Real vs. Rendered), and both OCR-based variants (OCR-1P and OCR-2P), evaluated across seven benchmarks: MMLU, ARC, GPQA, GSM8K, QASPER, SQuAD v2, and HumanEval. All results are reported as Accuracy or F1, except for **HumanEval**, which follows the standard **pass@1** metric. Accuracy values of QASPER and

In a dance class of 20 students, 20% enrolled in contemporary dance, 25% of the remaining enrolled in jazz dance, and the rest enrolled in hip-hop dance. What percentage of the entire students enrolled in hip-hop dance? Enclose only the final answer within <answer> and </answer>. Do not include any additional text inside the tags.

(a) Image format.

Text	In a dance class of 20 students, 20% enrolled in contemporary dance, 25% of the remaining enrolled in jazz dance, and the rest enrolled in hip-hop dance. What percentage of the entire students enrolled in hip-hop dance? Enclose only the final answer within <answer> and </answer>. Do not include any additional text inside the tags.
Instr. + Image	Please follow the instruction in the image. Enclose only the final answer within <answer> and </answer>. Do not include any additional text inside the tags. [Image provided in (a) without the format instructions.]

(b) Text and Instr. + Image format.

**Fig. S5:** An example input of GSM8K.**Table S1:** Dataset statistics and composition.

Dataset	Domain	Metric	#Samples	Proportion (%)
MMLU	Knowledge (57 subjects)	Acc.	14,042	83.0
ARC	Science reasoning	Acc.	1,172	6.9
GPQA	Graduate-level QA	Acc.	198	1.2
GSM8K	Math reasoning	Acc.	1,319	7.8
HumanEval	Code generation	Pass@1	164	1.0
QASPER	Document QA	F1 / Acc.	1,445	—
SQuAD v2	Reading comprehension	F1 / Acc.	100	—
<b>Total (synthetic-image benchmarks)</b>			<b>16,895</b>	<b>100.0</b>

SQuAD v2 are computed using the model-based evaluator described in Section F, ensuring consistent comparison across heterogeneous answer formats.

## F Evaluation for QASPER and SQuAD v2.

Standard EM or span-matching metrics are insufficient as a primary measure in our setting, since many answers are free-form, paraphrastic, or require multi-sentence justification. We therefore adopt a model-based evaluation for Accuracy: GPT-5 serves as an automatic judge and assigns a score of 1.0 (fully correct), 0.5 (partially correct), or 0.0 (incorrect) by comparing the model prediction against the reference answer. Accuracy is reported as the mean of these scores across all examples. In addition, we report the F1 used in prior work on QASPER and SQuAD v2. Concretely, answers are normalized (lowercasing, removing punctuation and articles), and F1 is computed as the harmonic mean of

precision and recall over overlapping tokens between the predicted and ground-truth answers, taking the maximum over multiple references when available.

## G FLOPs Analysis

To quantify the computational overhead of image-based inputs relative to text, we report the ratio of prefill FLOPs consumed by visual tokens to those consumed by text tokens for the same input. A higher ratio indicates that the image pathway demands proportionally more compute. As shown in Table S3, the ratio varies considerably across models and datasets. For short-context benchmarks (ARC, GSM8K, HumanEval, MathVista, MMLU) with a fixed rendered-image resolution, the ratio typically ranges from  $1.4\times$  to  $4.7\times$ , with Pixtral-12B being a notable outlier due to its higher native image-token count. For long-context datasets (SQuAD and QASPER), where the number of input images scales with document length, the ratio increases substantially, reaching up to  $29\times$  for Pixtral-12B on QASPER. These results highlight that, while visual inputs can provide richer structural signals, they come at a non-trivial computational cost that grows with document length.

## H OCR Quality and Task Accuracy

To investigate whether the visual recognition capability of each model explains the modality gap, we measure the correlation between OCR quality and task accuracy under the OCR-2Pass setting. For each model–dataset pair, we compute the Character Error Rate (CER) and Word Error Rate (WER) by comparing the OCR-extracted text against the gold text input. Figures S9a and S9b plot task accuracy against CER and WER, respectively.

The weak negative correlations ( $r = -0.279$  for CER,  $r = -0.238$  for WER) indicate that OCR quality alone does not account for the accuracy differences across models and datasets. While models with higher OCR error rates tend to have lower task accuracy, the relationship is far from deterministic: several models achieve high accuracy despite moderate OCR errors, and vice versa. This suggests that the modality gap is driven by factors beyond text recognition, including reasoning collapse and sensitivity to visual formatting.

Question:

When was King George's war?



Belligerents during the [Seven Years' War](#). Canadians and Europeans view the French and Indian War as a theater of the Seven Years' War, while Americans view it a separate conflict.

In [British America](#), wars were often named after the sitting British monarch, such as [King William's War](#) or [Queen Anne's War](#). There had already been a [King George's War](#) in the 1740s during the reign of [King George II](#), so British colonists named this conflict after their opponents, and it became known as the *French and Indian War*.<sup>[8]</sup> This continues as the

standard name for the war in the

United States, although [indigenous peoples](#) fought on both sides of the conflict. It also led into the Seven Years' War overseas, a much larger conflict between France and Great Britain that did not involve the American colonies; some historians make a connection between the French and Indian War and the Seven Years' War overseas, but most residents of the United States consider them as two separate conflicts—only one of which involved the American colonies,<sup>[9]</sup> and American historians generally use the traditional name. Less frequently used names for the war include the *Fourth Intercolonial War* and the *Great War for the Empire*.<sup>[8]</sup>

(a) Example input of Image format. Screenshot-based inputs lack complex visual hierarchy, making text-only reasoning nearly optimal.

Text	When was King George's war? The conflict is known by multiple names. In British America, wars were often named after the sitting British monarch, such as King William's War or Queen Anne's War. As there had already been a King George's War in the 1740s, British colonists named the second war in King George's reign after their opponents, and it became known as the French and Indian War. This traditional name continues as the standard in the United States, but it obscures the fact that Indians fought on both sides of the conflict, and that this was part of the Seven Years' War, a much larger conflict between France and Great Britain. American historians generally use the traditional name or sometimes the Seven Years' War. Other, less frequently used names for the war include the Fourth Intercolonial War and the Great War for the Empire. Enclose only the final answer within <code>&lt;answer&gt;</code> and <code>&lt;/answer&gt;</code> . Do not include any additional text inside the tags.
Instr. + Image	Please follow the instructions in the image. Enclose only the final answer within <code>&lt;answer&gt;</code> and <code>&lt;/answer&gt;</code> . Do not include any additional text inside the tags. [Image provided in (a) without the format instructions.]

(b) Text and Instr. + Image format.

Fig. S6: An example input of SQUAD v2.

Question:  
how did they measure grammatical correctness?

**Political Speech Generation**

**Vincent Kasarig**  
College of Information and Computer Sciences  
University of Massachusetts Amherst  
kasarig@umass.edu

**Abstract**

In this report we present a system that can generate political speeches for a desired political party. Furthermore, the system allows to specify whether a speech should hold a supportive or opposing opinion. The system relies on a combination of several state-of-the-art NLP methods which are discussed in this report. These include n-grams, Jurafsky & Katz FST big filter, recurrent neural networks, and latent Dirichlet allocation. Successes of words are generated based on probabilities obtained from two underlying models. A language model takes care of the grammatical correctness while a topic model aims for topical consistency. Both models were trained on the Corpus dataset which contains transcripts from US congressional floor debates. Furthermore, we present a manual and an automated approach to evaluate the quality of generated speeches. In an experimental evaluation generated speeches have shown very high quality in terms of grammatical correctness and sentence transitions.

**1 Introduction**

Many political speeches show the same structure and some characteristics regardless of the actual topic. Some phrases and arguments appear again and again and indicate a certain political affiliation or opinion. We want to use these reusable patterns to train a system that generates new speeches. Since there are major differences between the political parties we want the system to consider the political affiliation and the opinion of the intended speaker. The goal is to generate speeches where no one can tell the difference to hand-written speeches.

In this report we first discuss related works which deal with similar or related methods. Then we describe and analyze the dataset we use. Next, we present the methods we used to implement our system. We also describe the investigated methods that were not used in the final implementation. Then we describe a performed experiment and how we evaluated the results. Finally, we conclude our work and give an outlook. The appendix of this report contains the generated speeches from the experiment.

**2 Related work**

Creating models for a corpus that allow retrieving certain information is a major part of this project as well as in the entire NLP domain. Blei et al. [1] present in their paper a model which is known as latent Dirichlet allocation (LDA). LDA has become one of the most popular topic models in the NLP domain. LDA is generative probabilistic model that discovers automatically the underlying topics. Each document is modeled as a mixture of various topics. These topics can be understood as a collection of words that have different probabilities of appearance. Words with the highest probabilities represent the topics.

arXiv:1601.03313v2 [cs.CL] 20 Jan 2016

(a) The first image of Image format. The remaining pages are omitted for length considerations. All pages of the paper are fed into the model.

Text Question: how did they measure grammatical correctness?  
Political Speech Generation  
In this report we present a system that can generate political speeches for a desired political party. Furthermore, the system allows to specify whether a speech should hold a supportive or opposing opinion. The system relies on a combination of several state-of-the-art NLP methods which are discussed in this report. These include n-grams, ... [Full Paper Text]...  
Enclose only the final answer within <answer> and </answer>. Do not include any additional text inside the tags.  
Instr Please follow the instructions in the image. Enclose only the final answer + within <answer> and </answer>. Do not include any additional text inside Image the tags. [Image provided in (a) without the format instructions.]

(b) Text and Instr. + Image format.

Fig. S7: An example input of QASPER.

OCR Extraction Prompt.

You are an Optical Character Recognition (OCR) model. Your task is to extract all readable text from the provided image.

Instructions:

1. Identify and transcribe all visible text exactly as it appears, including numbers, punctuation, and symbols.
2. Preserve line breaks and spacing whenever possible.
3. For structured content (tables, forms, equations, lists), format using simple text notation:
  - Tables: use tabs or | separators between columns
  - Lists: use bullet points (-) or numbers
  - Equations: reproduce mathematical symbols faithfully
4. If a word or section is unclear, write [illegible] in its place.
5. Do not interpret, summarize, or translate the text—transcribe it exactly as shown.

Fig. S8: Prompt used for OCR-style transcription from images.

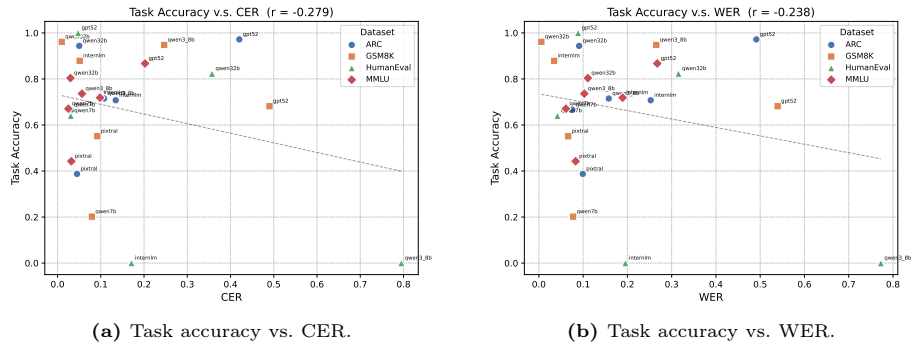


Fig. S9: Correlation between OCR quality and task accuracy under the OCR-2Pass setting. Each point represents one model–dataset pair. The dashed line shows the linear trend.

Dataset	Metric Model	Pure Text (T)	Instr.+Image (Real Image) (T+I)	Pure Image (Real Image) (I)	OCR-1P (T→I)	OCR-2P (I→T)	Pure Image (Rendered) (I)	Instr.+Image (Rendered) (T+I)	
MMLU	Acc.	GPT-5.2	92.33	-	-	86.54	86.72	90.93	91.06
		InternVL3-8B	59.83	-	-	0.37	71.86	33.93	69.09
		InternVL3.5-8B	63.97	-	-	68.99	80.75	62.27	63.70
		Pixtral-12B	37.89	-	-	0.66	44.25	42.76	41.60
		Qwen2.5-7B-VL	67.80	-	-	34.44	67.08	67.36	67.97
		Qwen2.5-32B-VL	78.34	-	-	76.55	80.38	73.79	75.47
Qwen3-8B	78.44	-	-	34.45	73.61	71.01	72.29		
Human Eval	Pass@1	GPT-5.2	100.00	-	-	98.17	100.00	100.00	71.34
		InternVL3-8B	56.71	-	-	0.00	0.00	45.12	71.95
		InternVL3.5-8B	90.24	-	-	84.76	86.59	89.02	90.24
		Pixtral-12B	39.02	-	-	0.00	0.00	47.56	79.27
		Qwen2.5-7B-VL	59.15	-	-	0.00	64.02	65.24	83.54
		Qwen2.5-32B-VL	31.10	-	-	0.00	82.32	85.98	22.56
Qwen3-8B	76.22	-	-	0.00	0.00	82.93	82.93		
ARC	Acc.	GPT-5.2	96.25	-	-	97.70	97.18	95.48	92.24
		InternVL3-8B	92.24	-	-	0.00	70.73	90.27	91.30
		InternVL3.5-8B	92.66	-	-	66.04	71.93	92.66	92.41
		Pixtral-12B	84.64	-	-	0.00	38.74	61.77	71.25
		Qwen2.5-7B-VL	87.20	-	-	34.47	66.55	89.42	85.92
		Qwen2.5-32B-VL	93.09	-	-	94.62	94.37	90.02	91.30
Qwen3-8B	91.72	-	-	44.11	71.50	91.04	91.38		
GSM8K	Acc.	GPT-5.2	95.83	-	-	77.86	68.16	96.51	85.14
		InternVL3-8B	78.01	-	-	0.00	87.87	42.53	49.51
		InternVL3.5-8B	95.30	-	-	87.64	94.47	95.30	95.22
		Pixtral-12B	3.79	-	-	0.00	55.12	8.11	4.93
		Qwen2.5-7B-VL	19.48	-	-	18.50	20.17	24.79	20.24
		Qwen2.5-32B-VL	95.07	-	-	0.00	96.13	94.92	4.47
Qwen3-8B	93.56	-	-	17.97	94.77	30.71	39.58		
GPQA	Acc.	GPT-5.2	81.25	-	-	77.90	80.58	80.13	81.25
		InternVL3-8B	33.71	-	-	30.58	33.26	32.81	32.14
		InternVL3.5-8B	42.63	-	-	40.18	46.21	34.60	40.40
		Pixtral-12B	31.25	-	-	29.69	30.36	27.23	30.36
		Qwen2.5-7B-VL	34.15	-	-	27.90	32.59	30.58	34.15
		Qwen2.5-32B-VL	42.41	-	-	43.08	43.30	43.97	41.52
Qwen3-8B	43.75	-	-	37.28	36.38	35.04	39.29		
QASPER (Full)	F1	GPT-5	29.18	29.36	28.28	-	28.89	29.76	27.25
		InternVL3-8B	21.60	16.32	12.51	-	15.51	16.27	10.84
		Pixtral-12B	-	-	-	-	-	-	-
		Qwen2.5-32B-VL-IT	11.41	11.46	12.88	-	12.08	11.46	13.40
	Qwen2.5-7B-VL-IT	10.07	24.39	10.28	-	19.43	24.31	19.26	
	Acc.	GPT-5	55.44	76.99	75.19	-	75.92	74.36	71.64
InternVL3-8B		48.14	69.38	55.26	-	56.40	62.97	46.28	
QASPER (Vis. Subset)	F1	GPT-5	25.56	29.64	29.61	-	29.19	30.15	27.86
		InternVL3-8B	17.78	16.91	13.07	-	15.54	16.71	11.20
		Pixtral-12B	-	-	-	-	-	-	-
		Qwen2.5-32B-VL-IT	12.06	12.13	10.70	-	12.92	11.55	10.44
	Qwen2.5-7B-VL-IT	10.60	25.44	19.45	-	20.73	24.26	19.14	
	Acc.	GPT-5	51.92	75.10	77.25	-	74.27	70.47	70.88
InternVL3-8B		44.02	69.36	54.43	-	56.15	62.57	44.64	
SQuAD v2	F1	GPT-5	77.82	67.87	71.69	67.11	64.77	-	-
		InternVL3-8B	32.80	32.42	24.93	18.68	26.43	-	-
		Pixtral-12B	72.73	31.64	19.43	31.87	31.34	-	-
		Qwen2.5-32B-VL-IT	13.89	25.91	20.07	26.12	24.37	-	-
	Qwen2.5-7B-VL-IT	6.77	25.79	27.09	30.25	29.51	-	-	
	Acc.	GPT-5	97.50	85.50	71.69	67.11	84.74	-	-
InternVL3-8B		82.50	84.00	73.50	76.50	69.50	-	-	
	Pixtral-12B	91.50	81.00	83.50	82.50	84.50	-	-	
	Qwen2.5-32B-VL-IT	86.50	84.00	87.00	83.00	83.50	-	-	
	Qwen2.5-7B-VL-IT	80.00	82.50	83.50	81.50	77.00	-	-	

**Note:** (T): text modality; (I): image modality. Accuracy and F1 are percentages. **QASPER (Full)**: all questions; **QASPER (Vis. Subset)**: figure/table-dependent questions.

**Table S2:** Performance comparison across input modalities on all seven datasets.

**Table S3:** Image-to-Text FLOPs ratio across models and datasets. A ratio of  $k$  indicates that processing the visual input requires  $k\times$  the FLOPs of processing the equivalent text input. Missing entries indicate that the model does not support the corresponding configuration.

Dataset	InternVL3-8B	Pixtral-12B	Qwen2.5-7B-VL	Qwen2.5-32B-VL	Qwen3-8B	Gemma3-4B
ARC	3.68	13.42	3.92	2.45	3.81	4.68
GSM8K	1.98	13.65	4.01	1.56	2.82	2.23
HumanEval	1.52	6.21	1.80	1.36	1.62	1.72
MathVista	3.03	14.67	4.39	1.68	3.28	4.52
MMLU	3.45	12.78	–	2.28	2.74	4.11
SQuAD	8.64	20.70	12.37	7.54	8.98	8.98
QASPER	8.33	29.29	9.38	5.91	6.50	1.80